A General Approach to Sizing and Power Density Equations for Comparison of Electrical Machines

Surong Huang, Jian Luo, *Student Member, IEEE*, Franco Leonardi, *Associate Member, IEEE*, and Thomas A. Lipo, *Fellow, IEEE*

Abstract—Whenever an electrical machine is meant to be fed by a power converter, the design should be approached as a system optimization, more than a simple machine sizing. A great variety of electrical machines is available to accomplish this goal, and the task of comparing the different options can be very difficult. A general purpose sizing equation, easily adjustable for every topology, that could take into account different waveforms and machine characteristics, would be a very desirable tool. In this paper, a general approach is presented to develop and to discuss such an equation. Sample applications of the sizing and power density equations are utilized to compare the induction machine and the doubly salient permanent magnet (DSPM) machine.

Index Terms—Ferrites, magnets, motors, power density, sizing equation.

I. INTRODUCTION

IN GENERAL, the comparison of different machine types is a very formidable task, since many variables exist for each machine and it is difficult to select those quantities which should be held constant and those that should be left free to vary. One traditional method of comparison is to use the $D_g^2 L_e$ sizing equation, which compares the machine power on the basis of the airgap volume, where D_g is the airgap diameter and L_e the effective stack length.

For many years, researchers have been interested in considering, instead, the machine outer diameter D_o, because it is more directly related to the volume and, thus, to the cost and size of the machine. In 1987, Honsinger developed a $D_o^2 L_e$ sizing equation for induction machines [1]. This method emphasized the importance of choosing the right electrical loading A on the machine optimization. Unfortunately, the approach leads to good designs only for small pole numbers, since optimizing $D_o^3 L_e$ is clearly not the same as optimizing $D_o^3 L_e$.

The traditional sizing equation is based on the assumption that the excitation of the machine is provided by a sinusoidal

voltage source, resulting in ac machines which produce a sinusoidal EMF. It was recognized in [2] and [3] that the emergence of power electronic converters has removed the need for such a concept as the basis for machine design. Beginning with the reluctance and brushless permanent magnet (PM) machine, a new phase of electrical machine design has been evolving, based on the principle that the best machine design is the one that simply produces the optimum match between the machine and the power electronic converter.

Given the great number of possible motor choices, it has become important to compare the power potential of machines with vastly different topologies and having a variety of different waveforms of back EMF and current. A systematic and easy-to-use method based on sizing equations is, therefore, very desirable to compare the capability of machines with different structures.

In order to eliminate the deficiencies of traditional sizing equations, this paper introduces special factors to account for the effect of nonsinusoidal current and back EMF waveforms. A particular effort is made to obtain a sizing equation which characterizes the output power P_R as a function of the overall volume of the machine. Thus, machines can be compared based upon the total occupied volume, instead of the airgap volume. The application of this general purpose sizing equation should provide machine designers with an important tool in their quest for new high-power density machines and structures.

II. SIZING EQUATIONS AND POWER DENSITIES

In general, if stator leakage inductance and resistance are neglected, the output power for any electrical machine can be expressed as

$$P_R = \eta \frac{m}{T} \int_0^T e(t)\,i(t)\,dt = \eta m K_p E_{\mathrm{pk}} I_{\mathrm{pk}} \qquad (1)$$

where EMF $e(t)$ and E_{pk} are the phase airgap EMF and its peak value. The currents $i(t)$ and I_{pk} are the phase current and the peak phase current, η is the machine efficiency, m is the number of phases of the machine, and T is the period of one cycle of the EMF. The quantity K_p is termed the electrical power waveform factor and is defined as

$$K_p = \frac{1}{T} \int_0^T \frac{e(t) \times i(t)}{E_{\mathrm{pk}} \times I_{\mathrm{pk}}}\,dt = \frac{1}{T} \int_0^T f_e(t) f_i(t)\,dt \qquad (2)$$

where $f_e(t) = e(t)/E_{\text{pk}}$ and $f_i(t) = i(t)/I_{\text{pk}}$ are the expressions for normalized EMF and current waveforms.

The peak value of EMF E_{pk} and the EMF itself $e(t)$ in (1) are given by

$$E_{\text{pk}} = K_e N_t B_g \frac{f}{p} D_g L_e \qquad (3)$$

and

$$e(t) = \frac{d\lambda_g(t)}{dt} = K_e N_t B_g \frac{f}{p} D_g L_e f_e(t) \qquad (4)$$

where Λ_g is the airgap flux linkage per phase, N_t is the number of turns per phase, f is the converter frequency, and p is machine pole pairs. The constant K_e is the EMF factor which incorporates the winding distribution factor K_w and the ratio between the area spanned by the (salient) poles and the total airgap area.

In order to indicate the effect of the current waveform, the definition of a current waveform factor K_i is also useful:

$$K_i = \frac{I_{\text{pk}}}{I_{\text{rms}}} = \left(\frac{1}{T} \int_0^T \left(\frac{i(t)}{I_{\text{pk}}} \right)^2 dt \right)^{-1/2} \qquad (5)$$

where I_{rms} is the rms phase current which is related to the stator electrical loading A_s, wherein

$$A_s = 2m_1 N_t \frac{I_{\text{rms}}}{\pi D_g} \qquad (6)$$

where m_1 is the number of phases of each stator (if there is more than one stator, each stator has the same m_1). The factor 2 is introduced here because N_t is the number of turns per phase, instead of the number of conductors per phase.

In the general case, the total electrical loading A should include both the stator electrical loading A_s and rotor electrical loading A_r, so that

$$A_s = A - A_r = \frac{A}{1 + K_\phi} \qquad (7)$$

where $K_\phi = A_r/A_s$ is the ratio of electrical loading on rotor and stator. In a machine topology without a rotor winding, $K_\phi = 0$.

Inserting (6) and (7) into (5),

$$I_{\text{pk}} = \frac{1}{1 + K_\phi} K_i A\pi \frac{D_i}{2m_1 N_t}. \qquad (8)$$

Combining (1), (4), and (8), the following $D_g^2 L_e$ sizing equation is obtained:

$$P_R = \frac{1}{1 + K_\phi} \frac{m}{m_1} \frac{\pi}{2} K_e K_i K_p \eta B_g A \frac{f}{p} D_g^2 L_e. \qquad (9)$$

In most radial airgap flux machines, the aspect ratio coefficient

$$K_L = \frac{L_e}{D_g} \qquad (10)$$

should be chosen based upon practical requirements of the application. Alternatively, in [4] and [5], an optimized range of the ratio of stack length versus pole pitch was given for conventional motors as a function of peak torque and temperature rise. From this data, through power regression, it is possible to obtain

$$K_L = \frac{\pi}{2} p^{-(2/3)}. \qquad (11)$$

However, this is clearly not the case for axial airgap flux machines, for which K_L must be carefully derived [6].

Inserting (10) into (9), it is possible to obtain a D_g^3 sizing equation:

$$P_R = \frac{1}{1 + K_\phi} \frac{m}{m_1} \frac{\pi}{2} K_e K_i K_p K_L \eta B_g A \frac{f}{p} D_g^3. \qquad (12)$$

To realize the required $D_o^3 L_e$ sizing equation, it is useful to define the ratio [1]

$$\lambda_o = \frac{D_g}{D_o} = f(d_{ss}, d_{cs}, L_{pm}, D_g, p) \qquad (13)$$

where d_{ss} is the depth of the stator slot, d_{cs} is the depth of the stator core, and L_{pm} is the length of the PM in the radial direction in the stator, if any. In general, the format of the function f will depend on the specific machine type, and it is impossible to derive a general format valid for every machine. A procedure needs to be developed to determine λ_o when studying a specific machine considering the effects of temperature rise, losses, and efficiency requirements. In practice, the depths d_{ss} and d_{cs} depend upon the stator electrical loading A_s, the current density J_s, the slot fill factor K_{cu}, and the flux density in the iron core. The length L_{pm} depends on the airgap flux density and airgap length, and the airgap surface diameter D_g is determined by (12).

The final general purpose sizing equation ultimately takes on the following form:

$$P_R = \frac{1}{1 + K_\phi} \frac{m}{m_i} \frac{\pi}{2} K_e K_i K_p \eta B_g A \frac{f}{p} \lambda_o^2 D_o^2 L_e. \qquad (14)$$

For convenience of design and for purposes of comparison, the corresponding D_o^3 sizing equation is found to be

$$P_R = \frac{1}{1 + K_\phi} \frac{m}{m_1} \frac{\pi}{2} K_e K_i K_p K_L \eta B_g A \frac{f}{p} \lambda_o^3 D_o^3. \qquad (15)$$

Finally, the machine power density for the total volume can be defined as

$$\xi = \frac{P_R}{\frac{\pi}{4} D_o^2 L_t} \qquad (16)$$

where L_t is the total length of the machine, including the stack length and the protrusion of the end winding from the iron stack in the axial direction.

By examining the back EMF and current waveform for a particular machine type, the factors K_i and K_p in the sizing equation can be determined. Several typical waveforms and their corresponding K_i and K_p are shown in Table I.

TABLE I
TYPICAL PROTOTYPE WAVEFORMS

Model	e(t)	i(t)	K_i	K_p
Sinusoidal waveform			$\sqrt{2}$	$\frac{1}{2}\cos\phi$
Sinusoidal waveform			$\sqrt{2}$	0.5
Rectangular waveform			1	1
Trapezoidal waveform			1.134	0.777
Triangular waveform			$\sqrt{3}$	0.333
Rectangular & Trapezoidal waveform			1.134	0.8
Rectangular & Trapezoidal waveform			1.389	0.556
Trapezoidal waveform			1.389	0.519
Rectangular & Triangular waveform			1.5	0.333
Rectangular waveform			1.225	0.667

TABLE II
VARIATION OF K (WITH RATED POWER FACTOR $\cos\phi_r$

$\cos\phi_r$	0.65	0.7	0.75	0.8	0.85	0.9	0.95
K_ϕ	0.74	0.77	0.82	0.86	0.9	0.95	0.985

TABLE III
RECOMMENDED VALUES OF B_g AND B_{ts} FOR
DIFFERENT SOURCE FREQUENCIES f

f (Hz)	40	50	60	80	200	400
B_{ts} (T)	1.68	1.56	1.48	1.35	1.00	0.80
B_g (T)	1.25	1.10	0.95	0.8	0.48	0.38

III. APPLICATION OF THE GENERALIZED SIZING EQUATION TO INDUCTION MACHINES

Considering the first sinusoidal back EMF and current waveforms inherent in induction machines (Table I, row 1), it is clear that $K_i K_p = (\sqrt{2}/2)\cos\phi_r$. For an induction machine, the factor $K_e = 2\pi K_w$. Then, from (14), the sizing equation of an induction machine is

$$P_{R(IM)} = \frac{\sqrt{2}\pi^2}{2(1+K_\phi)} \ K_w \eta \cos\phi_r B_g A \ \frac{f}{p} \ \lambda_o^2 D_o^2 L_e. \quad (17)$$

The corresponding power density of the induction machine is

$$\xi_{(IM)} = \frac{2\sqrt{2}\pi^2}{(1+K_\phi)} \ K_w \eta \cos\phi_r B_g A \ \frac{f}{p} \ \lambda_o^2 \frac{L_g}{L_t} \quad (18)$$

where $\cos\phi_r$ is the power factor which is related to the rated power $P_{R(IM)}$, the pole pairs p of the machine , and the converter frequency f. An estimate of $\cos\phi_r$ for the squirrel-cage motor is

$$\cos\phi_r = 1.07 \ P_R^{0.015} p^{-0.08} f^{-0.07}. \quad (19)$$

The above equation was verified through the NEMA-B squirrel-cage motor data, which were discussed in [5].

In an induction machine, K_ϕ is related to the rated power factor $\cos\phi_r$. In [7], a table (see Table II) was given to express the relationship between K_ϕ and $\cos\phi_r$.

Through power regression, an estimated equation for K_ϕ can be established as

$$K_\phi = 1.06 \ P_R^{0.0116} p^{-0.062} f^{-0.054}. \quad (20)$$

Choice of a proper airgap flux density B_g and stator tooth flux density B_{ts} is another important issue. Reference [5] offers a discussion of the relationship between B_{ts} and converter frequency f. From this source, the stator tooth flux density B_{ts} can be estimated reasonably by

$$B_{ts} = 5.47 f^{-0.32}. \qquad \%hbox(21)$$

In addition, Levi [8] has derived an optimal value for B_g expressed as

$$B_g = 0.5 \ K_{fe} B_{ts} K_{h1} \quad (22)$$

where K_{fe} is the stator lamination factor accounting for the air space between laminations. Note that symbol B_g here represents the fundamental component of airgap flux density, hence, K_{h1} is a factor to convert the airgap flux density waveform to its fundamental component; if the machine is not saturated and the airgap flux density has a sinusoidal waveform, then K_{h1} equals 1. If the machine is highly saturated and the airgap flux density has a nearly rectangular waveform, the factor K_{h1} will have a maximum value of $\pi/2$.

Table III shows some typical flux densities suggested for several converter frequencies.

In induction machines having an outer stator topology, the machine outer surface diameter D_o is given by

$$D_o = D_g + 2(d_{cs} + d_{ss}) \quad (23)$$

where d_{ss} is the depth of stator slot, d_{cs} is the depth of stator core given by

$$d_{cs} = \frac{B_g \alpha_p}{4 p K_{fe} B_{cs}} \ \pi D_g \quad (24)$$

where B_{cs} is the flux density in the stator core, and α_p is the ratio of average airgap flux density to peak airgap flux density.

The depth of the stator slot d_{ss} is

$$d_{ss} = \frac{2A_s}{K_{ds}J_sK_{cu}} = \frac{2A}{(1+K_\phi)K_{ds}J_sK_{cu}} \qquad (25)$$

where K_{ds} is the trapezoidal slot factor which is used to convert a trapezoidal slot to an equivalent rectangular slot for computational purpose.

Inserting (23)–(25) into the definition of λ_o [(13)] finally yields an equation for λ_o for the case of an induction machine having an outer stator radial airgap flux topology

$$\lambda_o = \frac{D_g}{D_o} = \frac{D_g}{D_g + 2d_{cs} + 2d_{ss}}$$
$$= \left(1 + \frac{\pi B_g \alpha_p}{2pK_{fe}B_{cs}} + 2K_{ss}\right)^{-1} \qquad (26)$$

where $K_{ss} = d_{ss}/D_g$.

Through a computational study, it is now possible to design a series of machines with different power ratings, pole pairs, and converter frequencies and to examine efficiency for various designs. To assure the reliability of such data, the results obtained from such a study were compared with published data on NEMA-B series motors, the efficiency of which can be approximated by

$$\eta = 0.7\, P_R^{0.03} p^{-0.025}\, f^{-0.01}. \qquad (27)$$

Of course, the efficiency of any electrical machine can be obtained by accurately calculating the losses in the machine. However, a detailed calculation of losses would unnecessarily complicate the sizing equation concept, which is intended to be a reasonably simple estimate of the machine size.

IV. APPLICATION OF THE GENERALIZED SIZING EQUATION TO DOUBLY SALIENT PERMANENT MAGNET (DSPM) MACHINES

The DSPM machine concept has been presented in [2] and [9]. For the DSPM topology (Figs. 1 and 2), it can be determined that $K_e = \pi$. Because there is no rotor winding, $K_\phi = 0$. The trapezoidal waveforms in Table I (row 8), are good approximations of the actual waveform and gives $K_iK_p = 0.721$. From (14), the following DSPM machines sizing equation is obtained:

$$P_{R(\text{DSPM})} = 0.361\, \pi^2 \eta B_g A\, \frac{f}{p}\, \lambda_o^2 D_o^2 L_e \qquad (28)$$

where the power density of the DSPM machine is

$$\xi_{(\text{DSPM})} = 1.444\, \pi \eta B_g A\, \frac{f}{p}\, \lambda_o^2 \frac{L_e}{L_t}. \qquad (29)$$

Due to the structure of the DSPM machine, the waveforms of the flux in different portions of the stator and rotor have different characteristics. In the stator teeth and the stator inner core, the flux has a unipolar pulsating waveform. In the stator outer core, a nearly constant flux exists. Only in the rotor teeth and core is there truly an ac flux.

It is very important to choose reasonable values of the flux density for the different portions of the DSPM machine. An optimization of such values will increase the power density of the machine and decrease the iron loss. After an in-depth computational study and optimization, it was found that the
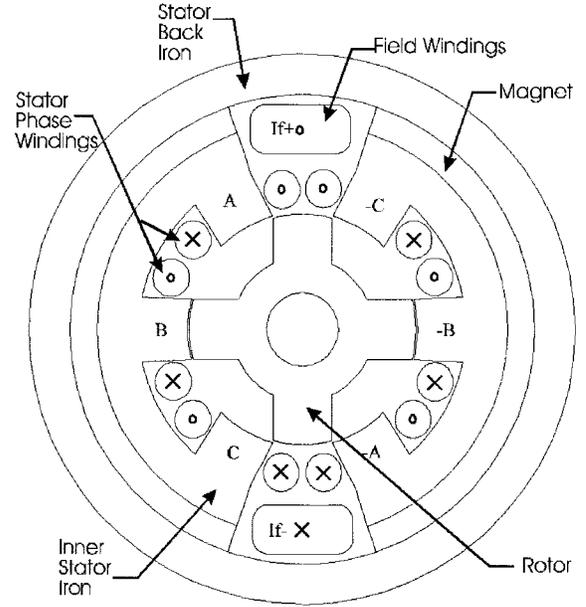

Fig. 1. DSPM4/6 machine with stator pole number $p_s = 6$, rotor pole number $p_r = 4$, and pole pairs $p = 4$.

flux density in stator teeth should be designed according to the following expression:

$$B_{ts} = \begin{cases} 2, & f \leq 20\ \text{Hz} \\ 5.47f^{-0.32}, & 20\ \text{Hz} < f < 60\ \text{Hz}. \\ 1.48 - (1.48 - 5.47f^{-0.32})/1.4, & f \geq 60\ \text{Hz} \end{cases}$$
$$(30)$$

Generally, the airgap flux density B_g and the rotor tooth flux density B_{tr} are specified to match B_{ts}. Based on the same numerical analysis, the flux density in the stator inner core should be

$$B_{cs1} = 1.48 - (1.48 - 5.47f^{-0.32}) \qquad (31)$$

and the flux density in the stator outer core

$$B_{cs2} = 1.4 \sim 1.8 \qquad (32)$$

where the value of B_{cs2} is chosen according to field weakening requirements.

The flux density in the rotor core is

$$B_{cr} = 4.38\, f^{-0.32}. \qquad (33)$$

In any PM machine, the airgap flux density B_g can also be expressed as

$$B_g = K_{\text{focus}}B_u \qquad (34)$$

where B_u is the attainable flux density on the surface of the PM's. The quantity K_{focus} is the flux-focusing factor, which is related to the structure of the PM machine and takes the form

$$K_{\text{focus}} = \frac{A_{pm}}{A_p}K_d \qquad (35)$$

where A_{pm} is the surface area of PM's, A_p is the area of the gap surface physically crossed by the flux, and K_d is the flux leakage factor of the PM machines obtained through a finite-element study or through design experience.
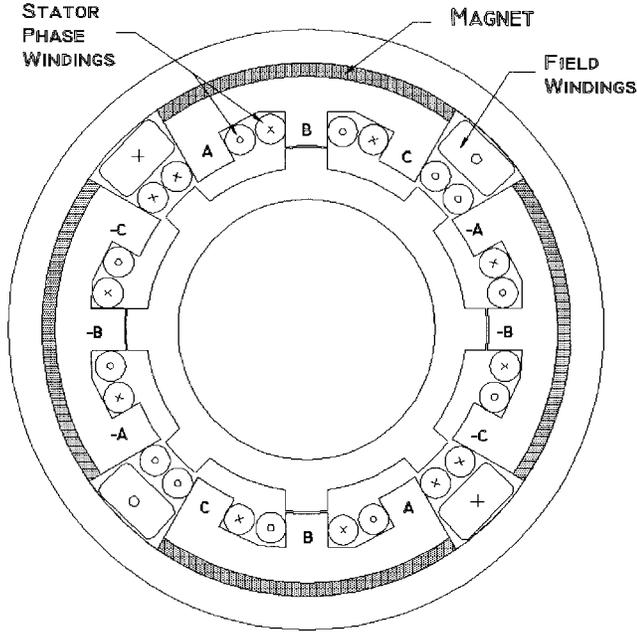
Fig. 2. DSPM8/12 machine with stator pole number $p_s = 12$, rotor pole number $p_r = 8$, and pole pairs $p = 8$.

Fig. 3. Power densities of four-pole IM and DSPM machines.

The optimal values of the aspect ratio coefficient K_L was given considering power density and efficiency and is, for DSPM4/6 machines, $K_L = 1.40 \sim 1.55$ and, for DSPM8/12 machines, $K_L = 0.65 \sim 0.75$.

In DSPM machines, the outer surface diameter D_o can be expressed as

$$D_o = D_g + 2(d_{cs1} + d_{cs2} + d_{ss} + L_{pm}) \qquad (36)$$

where d_{cs1} is the depth of the stator inner core given by

$$d_{cs1} = \frac{2\alpha_s}{2 + \alpha_s} \frac{B_{ts}}{B_{cs1}} \frac{\pi D_g}{p_s} \qquad (37)$$

and where α_s is the ratio of stator teeth portion to the stator pole pitch portion. For the structure shown in Figs. 1 and 2, where $\alpha_s = 0.5$, the quantity d_{cs2} is the depth of stator outer core given by

$$d_{cs2} = \frac{\alpha_s}{2} \frac{B_{ts}}{B_{cs2}} \frac{\pi D_g}{p_s}. \qquad (38)$$

The length of the PM is expressed as

$$L_{pm} = \frac{1.2\mu_r B_u}{0.95 B_r - \dfrac{B_u}{K_d}} K_{\text{focus}} g \qquad (39)$$

where B_r is the residual flux density of the PM material and g is the length of airgap. Reference [8] offers the following equation for estimating the airgap:

$$g = 4.7 \, 10^{-3} \, p^{-0.5} \, D_g. \qquad (40)$$

The depth of stator slot in the case of the DSMP is

$$d_{ss} = \frac{2A}{K_{ds} J_s K_{cu}}. \qquad (41)$$

Referring to the definition of λ_o [(13)] and the structure of the DSPM machine (Figs. 1 and 2), the inner-to-outer-surface-
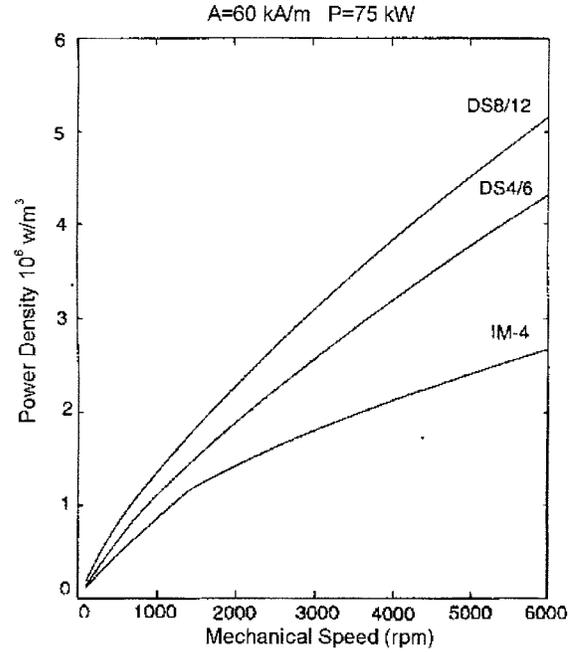
diameter ratio becomes

$$\lambda_o = \frac{D_g}{D_o} = \frac{D_g}{D_g + 2d_{cs1} + 2d_{cs2} + 2L_{PM} + 2d_{ss}}$$

$$= \left(1 + 0.8 \frac{B_{ts}}{B_{cs1}} \frac{\pi}{p_s} + 0.5 \frac{B_{ts}}{B_{cs2}} \frac{\pi}{p_s} + 1.128 \right.$$

$$\left. \cdot 10^{-2} \frac{\mu_r B_u}{0.95 B_r - \dfrac{B_u}{K_d}} K_{\text{focus}} p^{-0.5} + 2K_{ss} \right)^{-1}. \qquad (42)$$

Since DSPM machines are not widely used, the available data are insufficient to provide general expressions for the efficiency of such machines. A theoretical or a numerical approach is, therefore, necessary to give an estimate of their efficiency. The method adopted in this paper was to produce a number of computer generated designs, estimate the efficiency, and then utilize a power regression algorithm to obtain the efficiency equation. The estimated efficiency of the DSPM machines thus obtained is given by

$$\eta = 0.92 \, P_R^{0.01} p^{-0.015} f^{-0.01}. \qquad (43)$$

Again, calculating the total losses of DSPM machines directly will yield a more accurate estimate of efficiency.

V. COMPARISON BETWEEN INDUCTION AND DSPM MACHINES

It is now possible to calculate the power densities of induction machines and DSPM machines through the use of the sizing and power density equations. Fig. 3 shows the comparison of power densities among the four-pole induction machine (IM-4), the four-rotor-pole/six-stator-pole DSPM ma-

chine (DS4/6) and the eight-rotor-pole/12-stator-pole DSPM machine (DS8/12). The curves of Fig. 3 represent an interpolation between a great number of computer-generated machine designs. Each speed corresponds to a different machine which has its rated value at that point. The x axis should not be regarded as a speed range, but rather as rated speed. An effort was made to optimize the power density of each machine, achieving comparable, but not identical, efficiency and steady-state temperature. The comparison is based on the same current density, total current loading, and rated power. The induction machine (IM) motor data have been checked with available commercial products and appear to represent well the vast world of induction motors.

This study promises a power density improvement of nearly a factor of two for high-speed DSPM's over the induction motor. A slight efficiency penalty is expected at high speed because of DSPM8/12 has a relatively high pole number and, consequently, high flux frequency.

While corroborating test results cannot be included in this paper, some details on DSPM motor testing can be found in the literature [10]. More data are being collected and will soon be available.

VI. CONCLUSION

In this paper, the following results have been obtained.

1) A general purpose sizing and power density equation was developed in terms of the main machine dimensions $D_o^2 L_e$ instead of airgap dimensions $D_g^2 L_e$. This new approach permits a comparison of the capability of different machine topologies based upon the overall occupied volume.

2) Sample applications of the general purpose sizing and power density equation have been developed for both DSPM machines and IM's.

3) A powerful comparison tool for electrical machines has been presented, and common limitations of previous approaches have been eliminated.

4) A fair comparison between IM's and DSPM machines was attempted. The DSPM structure appeared to be capable of substantially higher power density than the equivalent induction machine.

REFERENCES

[1] V. B. Honsinger, "Sizing equations for electrical machinery," *IEEE Trans. Energy Conversion*, vol. EC-2, pp. 116–121, Mar. 1987.
[2] T. A. Lipo and Y. Li, "CFMs—A new family of electrical machines," in *Proc. IPEC'95*, Yokohama, Japan, Apr. 3–7, 1995, pp. 1-8.
[3] T. A. Lipo and F. X. Wang, "Design and performance of converter optimized AC machines," *IEEE Trans. Ind. Applicat.*, vol. IA-20, pp. 834–844, July/Aug. 1984.
[4] W. Schuisky, *Induktionsmaschimen.* Vienna, Austia: Springer-Verlag, 1957.
[5] T. A. Lipo, *Introduction to AC Machine Design*, Wisconsin Power Electronics Research Center, University of Wisconsin, Madison, WI, 1996.
[6] S. Huang, J. Luo, F. Leonardi, and T. A. Lipo, "A comparison of power density for axial flux machines based on the general purpose sizing equation," presented at the 1997 IEEE Power Engineering Society Summer Meeting, Berlin, Germany, July 20–24, 1997.
[7] S. Q. Chen, "Electrical machine design," Xian Jiaotong University, 1982, (in Chinese).
[8] E. Levi, *Polyphase Motors—A Direct Approach to Their Design.* New York: Wiley, 1984.
[9] Y. Li, F. Leonardi, and T. A. Lipo, "A novel doubly salient permanent magnet generator capable of field weakening," presented at the Conference on Design to Manufacture in Modern Industry (DMMI), Lake Bled, Slovenia, May 29–30, 1995.
[10] F. Leonardi, T. Matsuo, Y. Li, T. A. Lipo, and P. McCleer, "Design considerations and test results for a doubly salient PM motor with flux control," presented at the IEEE-IAS Annu. Meeting, San Diego, CA, Oct. 6–12, 1996.

Surong Huang was born in Shanghai, China. He received the B.S. and M.S. degrees in electrical engineering from Shanghai University, Shanghai, China.

From 1995 to 1996, he was a Visiting Faculty Member at the University of Wisconsin, Madison. He is currently an Associate Professor, College of Automation, Shanghai University. His research interests are motor and drive design, power electronics, and power systems.

Jian Luo (S'96) was born in Chengdu, China. He received the B.S. degree from Tsinghua University, Beijing, China, in 1984 and the M.S. degree from the First Academy of Aerospace Industry, Beijing, China, in 1987, both in electrical engineering. He is currently working toward the Ph.D. degree at the University of Wisconsin, Madison.

Prior to entering the Ph.D. program, he was an Electrical Engineer with the Beijing Institute of Control Devices, Beijing, China. His areas of interest include optimized electrical machine and drive design, modeling, and simulation.
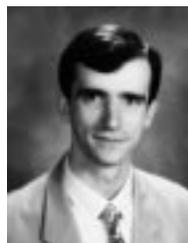
Franco Leonardi (S'93–A'95) received the Degree and the Doctorate degree in electrical engineering from the Universitá degli Studi di Padova, Padova, Italy, in 1991 and 1995, respectively.

From 1994 to early 1996, he was at the University of Wisconsin, Madison, where he was involved in research on synchronous reluctance and doubly salient permanent magnet motors. In 1996, he joined McCleer Power Inc., Jackson, MI, where he is currently engaged in the development of DSPM technology for traction applications and other research projects.

Thomas A. Lipo (M'64–SM'71–F'87) is a native of Milwaukee, WI. He received the Ph.D. degree from the University of Wisconsin, Madison, in 1968.

From 1969 to 1979, he was an Electrical Engineer in the Power Electronics Laboratory, Corporate Research and Development, General Electric Company, Schenectady, NY. He became Professor of Electrical Engineering at Purdue University, West Lafayette, IN, in 1979. In 1981, he joined the University of Wisconsin, Madison, where he is presently the W. W. Grainger Professor for Power Electronics and Electrical Machines.

Dr. Lipo has received the Outstanding Achievement Award from the IEEE Industry Applications Society, the William E. Newell Award of the IEEE Power Electronics Society, and the 1995 Nicola Tesla IEEE Field Award from the IEEE Power Engineering Society for his work. Over the past 30 years, he has served the IEEE in numerous capacities, including President of the Industry Applications Society.